Acta Geodyn. Geomater., Vol. 10, No. 1 (169), 111–120, 2013
DOI: 10.13168/AGG.2013.0011

SHAPE OPTIMIZATION OF FIBERS IN FRC

Petr P. PROCHÁZKA * and Martin VÁLEK

Department of Mechanics, Civil Engineeering, Czech Technical University in Prague, Thákurova 7, 166 29 Prague 6, Czech Republic
**Corresponding author's e-mail:* petrp@fsv.cvut.cz

(*Received* March 2012*, accepted* December 2012)

ABSTRACT

In this study shape optimization of fibers in composite fiber reinforced structure is presented. The problem targets the optimal shape with respect to the maximum bearing capacity and the minimum deformation of the whole composite set up. The shape is constrained by a constant volume (area) ratio. The optimization includes a process of seeking the overall properties of composites, i.e. localization and homogenization. Since no a priori estimate of the shape of fibers is known, numerical tool, finite element method, is employed. Such a problem is important in a wide range of applications, prevailingly in fiber reinforced concrete assessment, biomechanics, biophysics, and in the mechanics of classical composites with epoxy matrix. Since many types of fibers are used in various fiber reinforced concretes (fibers from polypropylene, steel, glass, clay, basalt, hemp, etc.), a deeper study is of importance to engineers and researchers. Application on FRC is preferred, i.e. fiber volume ratio is small, while classical composites require relatively very high volume ratio. The theory involves an original procedure leading to the optimal shape of fibers; it is then applied in the form of a numerical study. Also two examples from experiments verify the theoretical results. The problems are solved as two-dimensional, i.e. a unidirectional distribution of fibers is supposed.

KEYWORDS: fiber shape optimization, composites, fiber reinforced concrete, constrained volume (area)

1. INTRODUCTION

In this paper a classical problem of localization and homogenization is used for estimating an optimal shape of fibers in a composite structure. The properties of the material of both the fiber and matrix in the trial composite are known a priori, as they are required by the actual requirements of designer of the composite: fiber reinforced concrete. The optimal shape of fiber is sought in such a way that both minimum stress and deformation is attained. From the above arguments the only unknown is the shape of fibers. A constraint is applied to the area (volume) of the fiber, which is supposed to be constant for each distinguished case of iterative process solving the optimization problem. The constrained area of the fiber is involved into the formulation using Lagrangian multiplier, which is identified as a density of the surface energy along the interface of phases. Based on finite element method suiting for the solution of this problem the mathematical formulation is presented and after that an original numerical approach is outlined. The total energy of the system is minimized with respect to either displacements or stresses. The design parameters are beams led from the origin of the coordinate system centered in the unit cell. This problem requires star-shaped fibers. In experimental part results from tests with various cross-sections of fibers and various fiber volume ratios are mentioned.

In Oliver et al. (2012) and Kato et al. (2010) a minimization of suppressing damage along the interfacial boundary between fiber and matrix is studied. Such a problem is very close to that being solved in this paper. Both the latter studies consider the fibers in their main function, which is the bridging of fissures or cracks occurring along the tensile layers during bending of concrete beams. Note that the fiber reinforcement is very small in this case, i.e. the fiber volume ratio is about 1 %. On the other hand the application of fiber reinforcements of concrete can appear also in a bunker construction, protective walls, Szuladzinski (2012), aircraft shelters, Prochazka et al. (2011), etc. This is why this paper focuses on the composites with higher fiber volume ratios (0.04 to 0.07). In this context it is worth noting the paper by Cangiano et al. (2003) that optimizes the quality of the interfacial zone between the fiber and matrix.

In the presented paper the localization and homogenization procedures are first suggested, which basically follow the idea published by Suquet (1987). The idea is relatively old, but still it seems to be the most reliable in numerical treatment with composites.

Another approach leading to the effective material properties are based on introducing the polarization tensor that simplifies the description of the boundary conditions and domain fields; this can be found in Prochazka et al. (1996). It enables one to solve the problem in terms of boundary elements

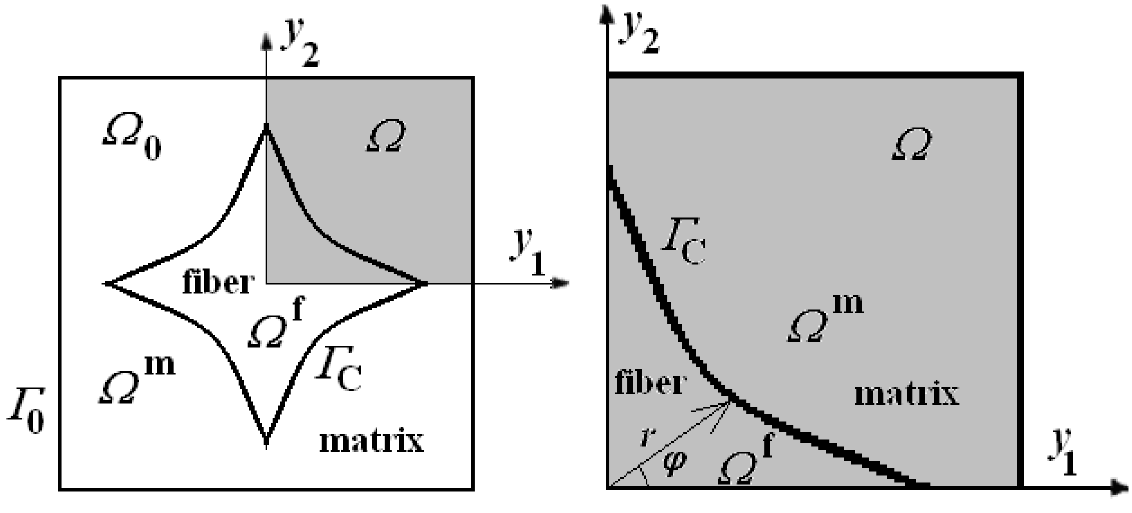

Fig. 1 Geometry of the unit cell and the domain the problem in which is solved.

which are probably the most efficient in solving this problem. The polarization tensor (or tensors) helps to ensure that uniform materials properties are extended from inside of the phases; this is a condition required in the boundary element procedures.

The process of optimization used in this paper is similar to that described in Prochazka et al. (2009), where it is applied to a problem of optimal distribution of thickness of various plates. Possible generalization to the optimization of debonding composites reveals in Kato et al. (2009) and Valek et al. (2009). The paper presented here differs from the other in the selection of the cost function, which appears to lead to more accurate results then in the case of functionals used previously.

For the practical use of the theory and applications paper by Prochazka et al. (2011) may serve, which provides users with concrete material properties, i.e. elastic coefficients like Young's moduly and Poisson's ratio.

Note that the self-sustained problem in this paper is quite newly formulated. First the idea of homogenization and localization is briefly described. As said before the approach of Suquet is employed leading to a well-posed problem (providing that the material properties of the phases are given), then the cost functional (function) is proposed and the Euler equations are formulated. From that, the optimization process is suggested. A set of examples addresses the most common cases emerging in practice.

The variables being denoted by the bold face letters are either vectors or higher order tensors. The colon means multiplication of matrices by vectors or matrices.

2. HOMOGENIZATION AND LOCALIZATION

In order to go into the core of the problem of the fiber shape optimization in fiber reinforced concrete with fibers of various material properties (given by the quality of the material properties of the fiber and matrix and by the ratio of the of phases), general procedure for homogenization and localization is briefly mentioned in what follows.

Let Ω_0 be a bounded domain describing the trial 2D unit cell, which is assumed as a square, for simplicity. The domain is equipped by either global (macro) coordinate system $0x_1x_2$ or local (micro) coordinate system $0y_1y_2$. In Ω_0 the conservation of momentum requires

$$\frac{\partial \mathrm{\sigma}}{\partial \mathrm{y}} = 0 \quad \left(\frac{\partial \sigma_{ij}}{\partial y_j} = 0,\ i,j = 1,2\right) \tag{1}$$

and the linear Hooke law is valid as,

$$\mathrm{\sigma} = \mathrm{L} : \mathrm{\varepsilon} \quad (\sigma_{ij} = L_{ijkl}\varepsilon_{kl},\ \ i,j,k,l = 1,2) \tag{2}$$

where the standard notation of tensor products and tensor differentiation is used with upright writing tensor notation.

Tensors $\mathrm{\sigma} = [\sigma_{ij}]_1^2$, $\mathrm{\varepsilon} = [\varepsilon_{ij}]_1^2$, $\mathrm{y} = (y_1, y_2)$ denote the stress tensor, the strain tensor and the point coordinate, respectively.

The relations between both the local and macro levels are given as the Lebesque measures on the unit cell Ω_0, i.e.

$$\begin{aligned} \Sigma_{ij} &= \frac{1}{\operatorname{meas}\Omega_0} \int_{\Omega_0} \sigma_{ij}(\mathrm{y})\, \mathrm{d}\Omega_0, \\ E_{ij} &= \frac{1}{\operatorname{meas}\Omega_0} \int_{\Omega_0} \varepsilon_{ij}(\mathrm{y})\, \mathrm{d}\Omega_0 \end{aligned} \tag{3}$$

where Σ_{ij} are components of the overall stress tensor, E_{ij} are components of the overall strain tensor and meas stands for measure; in most cases the measure of Ω_0 is one. From (2) it is obviously seen that while the components of the stress and strain tensors are dependent on the position at the micro level the appropriate overall variables are independent on x . On the other hand the unit cell is cut out of the composite and it represents not only the point x but also its neighborhood, so it means that the conditions inside of the unit cell can change from point to point in the whole composite. A typical set up of a unit cell considered is depicted in Figure 1.

The aim of the homogenization is to determine the relation $\Sigma = \mathrm{L}^* : \mathrm{E}$, where L^* is the overall stiffness tensor. In our problem L^* is sought to deliver the best material properties obeying the requirement of the maximum bearing capacity and in the same time the minimum of displacements.

Because of symmetry, let us consider only the first quarter Ω , see Figure 1.

Let E_{ij} be successively given as unit impulses, i.e. select i_0, j_0 from the set of integers (1,2), $E_{i_0 j_0} = 1$ and $E_{ij} = 0$ for $i \neq i_0$ and $j \neq j_0$. Substituting into (3) the weak formulation is easy to obtain and the finite element solution for $\mathrm{u}^* \in [H^1(\Omega)]^2$ can be found.

Necessary boundary conditions are shown in Figures 2 to 4.

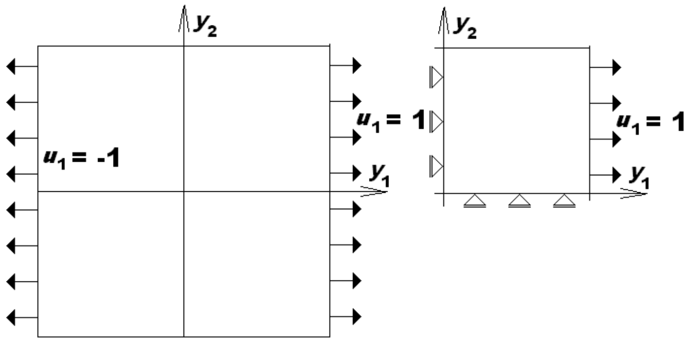

Fig. 2 Original and computational model for responses of E_{11}.

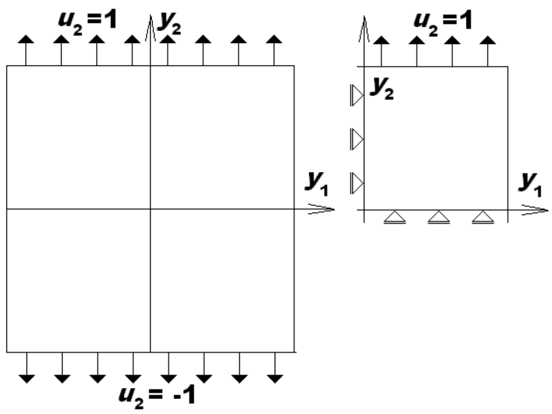

Fig. 3 Original and computational model for responses of E_{22}.

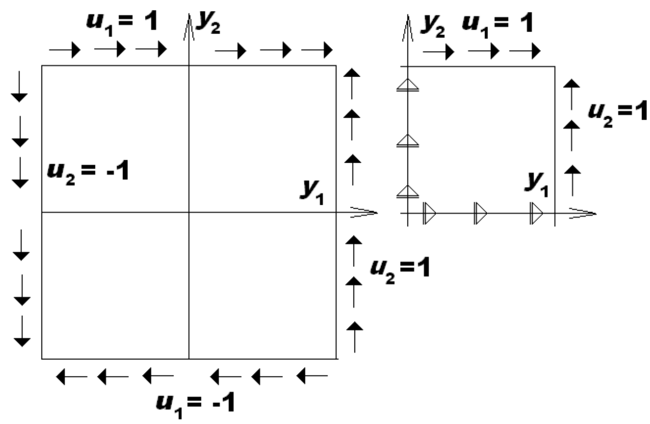

Fig. 4 Original and computational model for responses of E_{12}.

The partial solutions lead to the influence tensors (fourth-order "concentration factor tensors") $\mathrm{A}^{\mathrm{m}}, \mathrm{A}^{\mathrm{f}}$, and consequently to $\mathrm{B}^{\mathrm{f}}, \mathrm{B}^{\mathrm{m}}$, which are constructed from the successive relations:

$$\varepsilon_{ij}^{p}(\mathrm{u}^{*}(\mathrm{y})) = \beta_{ijkl}^{p}(\mathrm{y}) E_{kl}\,,$$
$$\varepsilon_{ij}^{p}(\mathrm{u}(\mathrm{y})) = (I_{ijkl} + \beta_{ijkl}^{p}(\mathrm{y})) E_{kl} = A_{ijkl}^{p}(\mathrm{y}) E_{kl}\,,$$
$$c^{\mathrm{f}} < \mathrm{A}^{\mathrm{f}} >_{\mathrm{f}} + c^{\mathrm{m}} < \mathrm{A}^{\mathrm{m}} >_{\mathrm{m}} = \mathrm{B}^{\mathrm{f}} + \mathrm{B}^{\mathrm{m}} = \mathrm{I}$$
$$< . >_{p} = < . >_{\Omega^{p}} \tag{4}$$

where
the superscript $p \equiv \mathrm{f}$ for $\mathrm{y} \in \Omega^{\mathrm{f}}$, $p \equiv \mathrm{m}$ for $\mathrm{y} \in \Omega^{\mathrm{m}}$, I is the unit fourth-order tensor and c^{f} and c^{m} are the appropriate volume fractions. Finally, the overall Hooke's law and the overall stiffness tensor are found as,

$$\Sigma_{ij} = [L_{ijkl}^{\mathrm{f}} B_{kl\alpha\beta}^{\mathrm{f}} + L_{ijkl}^{\mathrm{m}} B_{kl\alpha\beta}^{\mathrm{m}}] E_{\alpha\beta} =$$
$$= [(L_{ijkl}^{\mathrm{f}} - L_{ijkl}^{\mathrm{m}}) B_{kl\alpha\beta}^{\mathrm{f}} + L_{ij\alpha\beta}^{\mathrm{m}}] E_{\alpha\beta}, \tag{5}$$
$$L_{ijkl}^{*} = [(L_{ijkl}^{\mathrm{f}} - L_{ijkl}^{\mathrm{m}}) B_{kl\alpha\beta}^{\mathrm{f}} + L_{ij\alpha\beta}^{\mathrm{m}}]$$

3. OPTIMIZATION FOR MINIMUM TOTAL STRAIN ENERGY

The formulation of the cost functional will be done in terms of the constrained total energy. This formulation is elegant, as it covers the solution of the problem of the linear elasticity for an arbitrary fiber shape and, moreover, it leads to the minimum stresses and the minimum displacements as well, see, Prochazka et al. (2009). Since, on the other hand, the internal energy and the external energy are identical the energy density calculated for a specific case delivers the results given by either the displacement or the traction on the surface $\partial\Omega_0 \equiv \Gamma_0$ if the dual variable remains the same for all cases of iterative process.

One of natural questions for engineers dealing with composites could be: determine such a shape of fibers that the bearing capacity of the entire composite structure increases and attains its maximum. It means that the stresses are minimized in the domain Ω, their excesses are suppressed, and even the displacements reach the minimum. This is a problem of optimal shape of structures and can be formulated for composites as follows: Let the uniform strain fields E_{kl} (components of unit impulses of the overall strain tensor) are applied in the domain Ω (in our case successively the unit displacements are applied along the boundary of the unit cell, see Figs. 2 to 4). This produces concentration factors A_{mnkl}^{f} and A_{mnkl}^{m} as described in the second section. Let $\Pi(\mathrm{A}^{\mathrm{f}}, \mathrm{A}^{\mathrm{m}}, \Omega^{\mathrm{f}}, \Omega^{\mathrm{m}})$ be a real functional of A_{mnkl}^{f}, A_{mnkl}^{m} and $\Omega^{\mathrm{f}}, \Omega^{\mathrm{m}}$. Our problem of optimal shape consists of finding such a domain Ω^{f} from a class $O \equiv \{\Omega^{\mathrm{f}}; \text{measure } \Omega^{\mathrm{f}} = c^{\mathrm{f}}\}$ of admissible domains, where C is a constant, which minimizes Π.

Let us concentrate on the construction of the functional. First, the Hill lemma is valid; see e.g. Suquet (1987):

$$\int_{\Omega_0} \sigma_{ij}(\mathrm{y}) \varepsilon_{ij}(\mathrm{y})\, \mathrm{d}\Omega = S_{ij} E_{ij} \tag{6}$$

Since it holds $\Omega_0 = \Omega^{\mathrm{f}} \cup \Omega^{\mathrm{m}}$, one can consider only Ω^{f} as a representative of Ω^{m}, because of (4). Moreover, the concentration factors are depend on displacement u. The admissible class O involves the star shaped areas and the beams identifying the domain of the fiber are restricted in such a way that they do not cross Γ_C and $\partial\Omega$. The Lagrangian involving the side condition using the Lagrangian multiplier is written as:

$$\Pi(\mathrm{u}, \Omega^{\mathrm{f}}(\mathrm{r})) = \frac{1}{2} \int_{\Omega_0} \sigma_{ij}(\mathrm{y}) \varepsilon_{ij}(\mathrm{y})\, \mathrm{d}\Omega + \lambda\Big(\int_{\Omega^{\mathrm{f}}} \mathrm{d}\Omega^{\mathrm{f}} - C\Big) =$$
$$= \frac{1}{2} S_{ij} E_{ij} + \lambda\Big(\int_{\Omega^{\mathrm{f}}} \mathrm{d}\Omega^{\mathrm{f}} - C\Big) \tag{7}$$

owing to Hill's energy condition (6). Coefficient λ is a Lagrangian multiplier. Substituting (4) and (5) to (7) gives:

$$\Pi(\mathrm{u}, \Omega^{\mathrm{f}}(\mathrm{r})) = \frac{1}{2}[L_{ijkl}^{\mathrm{f}} < A(\mathrm{r})_{kl\alpha\beta}^{\mathrm{f}}(\mathrm{y}) >_{\mathrm{f}} + L_{ijkl}^{\mathrm{m}} < A(\mathrm{r})_{kl\alpha\beta}^{\mathrm{m}}(\mathrm{y}) >_{\mathrm{m}}] \cdot$$
$$\cdot E_{ij} E_{\alpha\beta} + \lambda\Big(\int_{\Omega^{f}} \mathrm{d}\Omega^{\mathrm{f}} - C\Big) \tag{8}$$

or

$$\Pi(\mathrm{u}, \Omega^{\mathrm{f}}(\mathrm{r})) = \frac{1}{2}[(L_{ijkl}^{\mathrm{f}} - L_{ijkl}^{\mathrm{m}}) B_{kl\alpha\beta}^{\mathrm{f}}(\mathrm{r}) + L_{ij\alpha\beta}^{\mathrm{m}}] \cdot$$
$$\cdot E_{ij} E_{\alpha\beta} + \lambda\Big(\int_{\Omega^{f}} \mathrm{d}\Omega^{\mathrm{f}} - C\Big) \tag{9}$$

and the concentration factors are dependant only on vector r. Even, only one of the two has to be calculated, which belongs to the fiber area, for example.

3.1. EULER'S EQUATIONS

First, differentiating (9) by u (Gateaux derivative) reveals the standard Lagrange variational principle, which describes the behavior of displacements, strains and stresses inside of the domain Ω (or Ω_0). This problem is to be solved in each iteration and for each unit impulse of the movements of beams r_s. The problem is solved for external loading given by unit displacements on the boundary $\partial\Omega$ (Figs. 2 to 4).

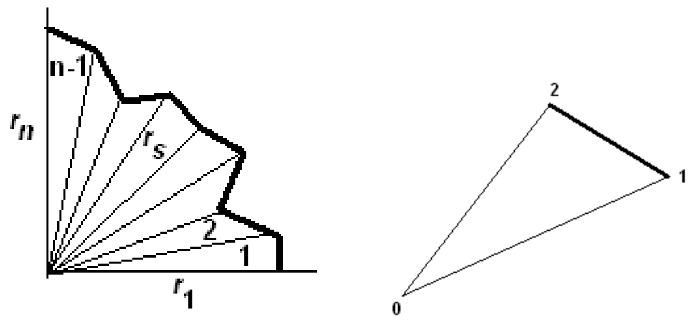

Fig. 5 Sample triangulation of fiber and a typical triangle.

The stationary statement leads to a differentiation of the functional by the shape (design) parameters r_s

$$\frac{\partial \Pi(\mathrm{u}, \Omega(\mathrm{r}))}{\partial r_s} = \frac{1}{2}[(L^{\mathrm{f}}_{ijkl} - L^{\mathrm{m}}_{ijkl})\frac{\partial}{\partial r_s} B^{\mathrm{f}}_{kl\alpha\beta}(\mathrm{r})] \cdot \\ \cdot E_{ij} E_{\alpha\beta} + \lambda \frac{\partial}{\partial r_s} \int_{\Omega^f} \mathrm{d}\Omega^{\mathrm{f}} = 0 \tag{10}$$

which can be rewritten as:

$$E_s + \lambda = 0, \quad s = 1,2,...,n \tag{11}$$

where

$$\lambda = \frac{\frac{1}{2}[(L^{\mathrm{f}}_{ijkl} - L^{\mathrm{m}}_{ijkl})\frac{\partial}{\partial r_s} B^{\mathrm{f}}_{kl\alpha\beta}(\mathrm{r})] E_{ij} E_{\alpha\beta}}{\frac{\partial}{\partial r_s} \int_{\Omega^f} \mathrm{d}\Omega^{\mathrm{f}}}$$

for each $s = 1,\ldots,n$

and n is the number of DOF on Γ_C.

It remains to state the design parameters r identifying the change of the boundary Γ_C of the fibers. If r_s, $s = 1,...,n$ are the distances of the origin from the current boundary of the fiber at point $y_s \in \Gamma_C$, symbol E_s corresponds to the strain energy density at the point of the interfacial boundary, in our case at the nodal point ξ_s. Eq. (11) requires E_s to have the same value for any s. In other words, if the strain energy density E_s were the same at any point on the "moving" part of the boundary Γ_C, the optimal shape of the trial body would be reached.

The approximation of the final value of E is calculated as the arithmetical average of the calculated E_s, i.e.

$$E = \sum_{s=1}^{n} E_s / n, \quad \delta = c(E - E_s)/E \quad c \text{ is the step} \tag{12}$$

It appears that the excesses of δ are not too large, as is in the case of optimization of beams, Prochazka et al. (2009). There the logarithmic scale is used instead and the average has to be used instead of arithmetic average (12). The movements of the beams r_s are improved according to the rule, which says that the bigger difference δ the shorter beams r_s are appropriate. From practical examples it is recognized that this algorithm is very fast and delivers reliable results.

Differentiating by λ completes the system of Euler's equations (T_s are triangles created by the origin and the boundary element on Γ_C, i.e. abscissa connecting two adjacent interfacial boundary nodal points):

$$\sum_{s=1}^{n} \text{meas } T_s = C \tag{13}$$

In order to calculate the current area, a sample triangulation of the fiber used in this study is depicted in Figure 5.

The area of each triangle is calculated according to the well known formula:

$$\text{meas } T_s = \frac{1}{2} \det \begin{bmatrix} 1 & 1 & 1 \\ y_1^0 & y_1^1 & y_1^2 \\ y_2^0 & y_2^1 & y_2^2 \end{bmatrix}$$

It is obvious from the later relation that constant E_s remains the same for each admissible s. It appears that if r is too long then E is too small and vice versa. This conclusion offers a very efficient algorithm for the optimization. For more details see Prochazka et al. (2009), where beam problems are solved.

It still remains to improve the area, which after differentiation by r_s can be different from required C. It is immediately seen that a standard quadratic collinear mapping can be applied to get the desired area.

3.2. EXAMPLE

Since finite element method serves a numerical tool one can expect that the mesh of the unit cell influences the results significantly. In these numerical

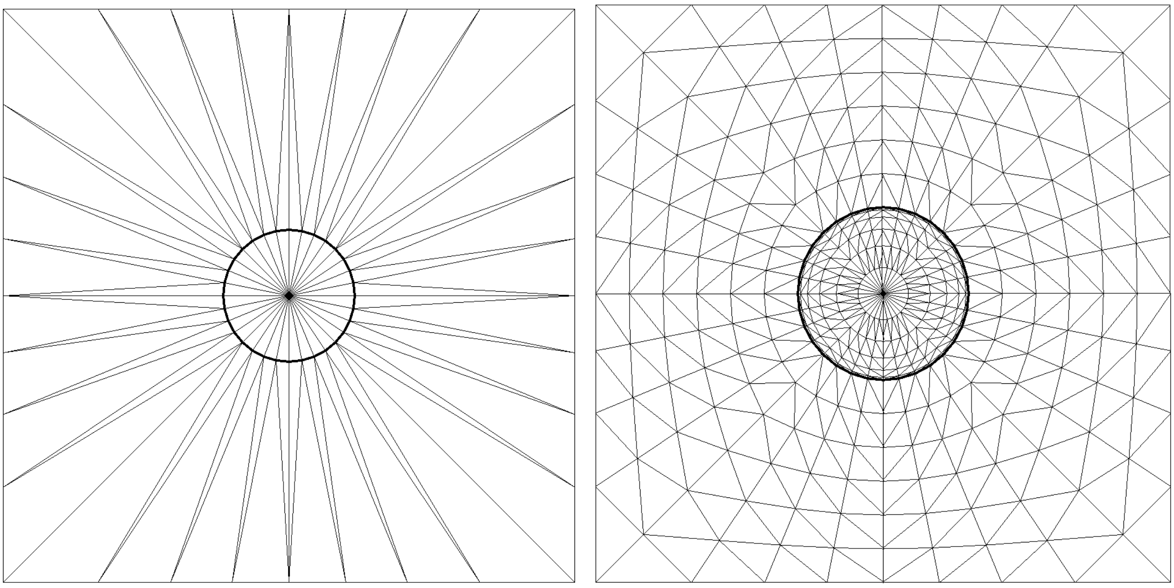

Fig. 6 Starting meshes fiber ratio 0.0415 $\times$0.07.

studies it appears that in some cases it is true and in others this dependence of results of the optimal shape of fibers is relatively small. Two typical cases are selected concerning the material properties. In the first case a stiffer fiber and a weak matrix are observed and in the second case the reverse material properties are considered, i.e. stiff matrix and weak fibers are contemplated. In all combinations of material properties the stiffer medium is identified by modulus of elasticity $E = 30000\,\text{ksi} = 210\,\text{GPa}$ and Poisson's ratio $\nu = 0.16$ while the weaker medium is defined by modulus of elasticity $E = 2430\,\text{ksi} = 17\,\text{GPa}$ and $\nu = 0.3$. The unit cell is always 1×1 mm^2 and the starting geometry of the fiber, positioned symmetrically in the cell, is circular, as seen from Figure 6. Three typical lay ups of the fibers embedded into the matrix are studied with various meshes.

The constrained beams of nodal points describing the interfacial boundary between fiber and matrix are selected as:

1. $r(\phi) \geq a = 0.1$ mm, $0 \leq \phi \leq 2\pi$ (the lower bound means that no nodal point of the interfacial boundary between the fiber and matrix can be too close to the singular point centered at the origin of local coordinates)
2. $r(\phi)/\cos\phi \leq d = 0.1$ mm, $0 \leq \phi \leq 2\pi$ (the upper bound means that the nodal points of the interface cannot be too close to the external boundary of the unit cell).

In all cases studied in what follows the fine mesh is considered the best FEM approximation. The results attained on the course mesh are shown for comparison and possible estimate of sensitivity.

In Figure 6 the starting meshes are shown, the left one is an example of the course mesh for the fiber volume ratio of 0.0415 and the right one is the best starting mesh considered in this paper for the fiber volume ratio of 0.07.

In Figure 6 a comparison between the results from examples of stiffer matrix (left picture) and stiffer fiber (right picture) is seen. Here the starting radius of fiber is 0.115, i.e. the fiber ratio is 0.0415. It appears that the shape of the first case (stiffer matrix) is very similar to that attained in Figure 7 for higher fiber volume ratio. Moreover, there is no danger for appearing nodes on Γ_C approaching the lower constraint 1), not speaking about violating the constraint 2) (because the fibers are too small). The interchange of the material properties leads us to interesting conclusions. First, there are "touch nodes" with the obstacle given by the lower constraint 1), i.e. there are the nodal points in contact with the fictitious circle given by the constraint 1). It probably causes that, in comparison to the previous case, the shape of interfacial boundary is wavier. An "internal iteration" has to be carried out for improvement of the "touch nodes". The internal iteration is carried out to fulfill the constraint condition on the constant fiber volume ratio. That one is very fast and do not cause any trouble as for the increase of time consumption.

In Figure 8 the starting radius of the interface line is 0.15 mm, so that all nodal points are far from the obstacle given by the constraint 1) and the internal iterations are to be expected in an ample range (no additional collinear mapping necessary to apply). The fiber ratio is 0.07. In case the weaker matrix is assumed almost rectangular shape seems to be optimal. In comparison with the case of fiber ratio 0.0415 the shape of fiber seems to be more circular, and for higher volume ratio the shape approaches the circle. For stiffer fiber again significant vertices are observed, i.e. Dramix type fibers are of optimal shape.

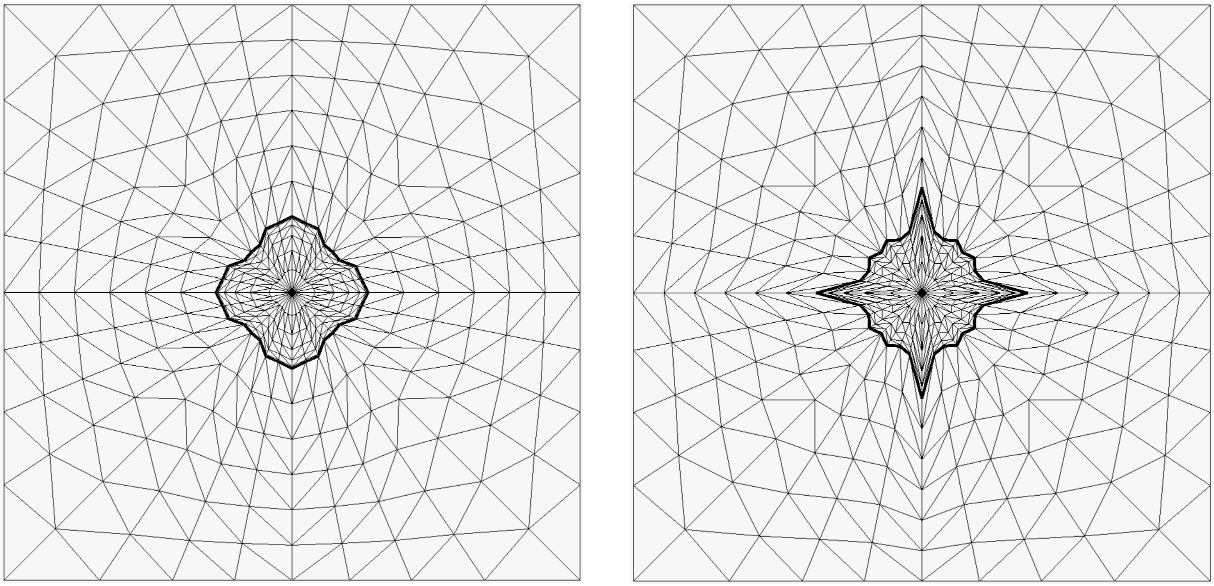

Fig. 7 Fiber ratio 0.0415, stiff matrix × stiff fiber.

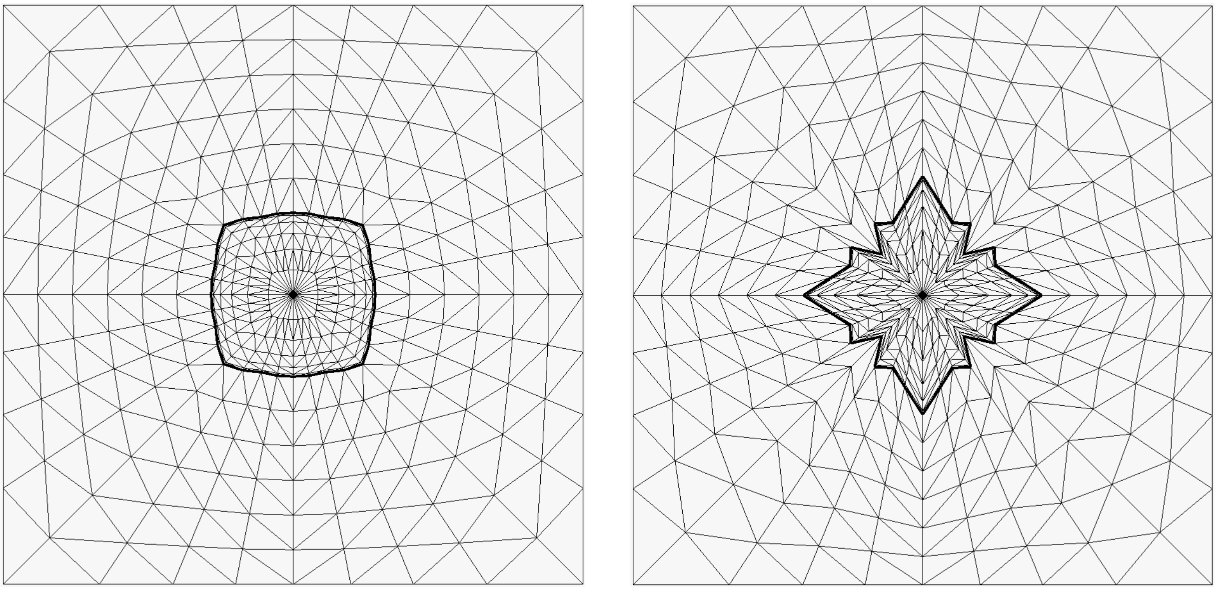

Fig. 8 **F**iber ratio 0.07: stiff matrix × stiff fiber.

Figure 9 provides us with comparison between fine and coarse meshes. The resulting shapes change in details, but the nature of the shape of fibers remains almost unchanged. More or less, the lower obstacle (fictitious circle, condition 1)) affects the shape slightly. The number of beams defining the nodal points of interface slide during the iteration is the same manner in both cases depicted in Figure 9. It is of interest to us that here, although couple of points is in a contact with the fictitious circle identifying the lower constraint 1), the change of the shape is not decisive when applying the fine mesh.

Considering another example where optimal holes (the stiffness tensor of the fiber is put equal to zero tensor) are monitored in a unit cell the following picture can be drawn for various fiber volume ratios (Fig. 10). This example is not directly connected with the problem of FRC but shows us that either greater or smaller fiber volume ratio there is no basic change of the character of the optimal shapes from the point of view of numerical results.

4. EXPERIMENTS

The optimization problems described in this article deal with an optimal shape of fibers in fiber reinforced concrete. It is of great importance to us at which stage of curing process the optimization should take place. Such a study is not covered here. This is

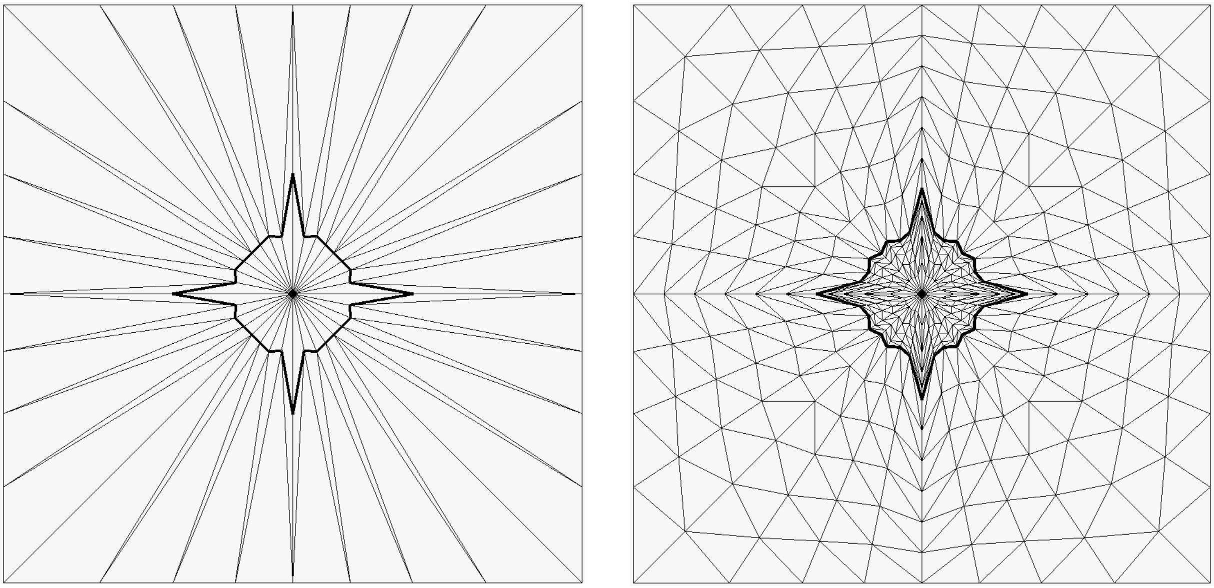

Fig. 9 Fiber ratio 0.0415, stiff fiber, course × fine meshes.

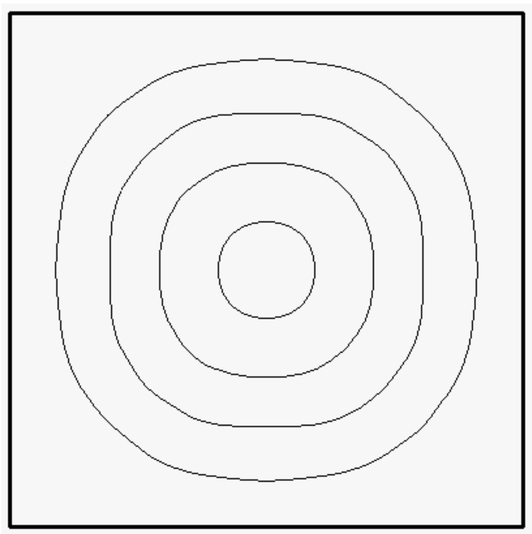

Fig. 10 Optimal shape of holes for various volume fractions.

why a large extent of tests has been carried out for fiber reinforced concretes, which are reinforced by standard fibers with rectangular cross-sections and the Dramix type fibers (adapted as straight fibers) with optimal cross-section and the results are compared. In both cases steel fibers are used as the reinforcement.

Testing machine MTS Alliance RT/30, see Figure 11 is used for the tests having been carried out for the purpose of this study. It is an electromechanical tool for compressive, tensile, and bending tests of material. Maximum compressive and tensile force is 30kN. The size of possible samples is 150 x 150 x 250 mm (width x length x height). The velocity of loading was in our case 0.04 mm/minute.

The scheme of the samples fiber-concrete aggregate in which has been tested is depicted in Figure 11. In the container the cement paste with embedded one fiber to five fibers symmetrically positioned in the aggregate is pored and cured. Three samples have been tested for the optimal shape of fibers (Dramix type) and another three samples had standard rectangle's fibers. The steel fibres with a diameter of 0.095 mm, length of 80 mm were used for laboratory tests.

Specimens of the rectangular or Dramix shapes with diameter 30 mm and height of 50 mm were made (Fig. 11). During the preparation of specimens, one to five steel fibres were placed into the cement mixture in the cylinder, considered as a representative volume element, so as 50 mm of fibre lies in the specimen and remaining part of 30 mm serves for fibre fixation in the grip installed in the measuring device. When one fibre was used, it was placed in the centre of the specimen, two to five fibres were placed in the plane passing through the centre of the specimen, symmetrically to the centre. The distance between fibres was 5 mm. The experiment was prepared with high quality of preparation of cement pasta and the positioning of the fiber was also extraordinarily accurate. The results of this study testify for this, as the variance is very small.

In the last stage of curing after 28 days pullout tests were carried out with the aim to get σ - ε (force-displacement) relations for all five samples. The results are seen from Table 1. Almost linear behavior before reaching the peak value testifies for brittle behavior at the fiber-matrix contact. The toughness of the aggregate is surprisingly high in both cases. Also brittle material behavior is seen from the pictures, although bearing of the aggregate persist to the nonlinear zone.

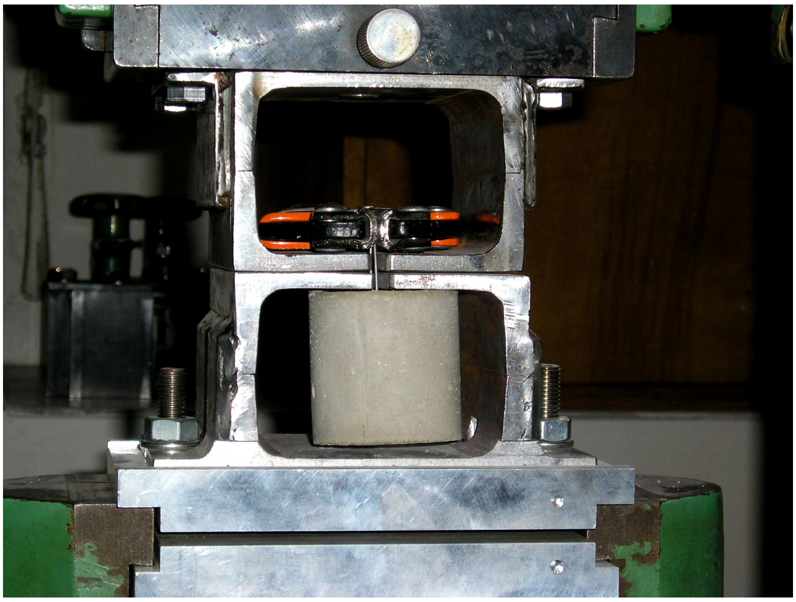

Fig. 11 Loading machine with adapted jaws.

Table 1 Comparison of limit pull-out force.

Fiber ratio	1 %	2.5 %	4 %	5.5 %	7 %
Dramix straight fibers [N]	383.33	800	1192	1774	1907.5
Rectangular straight fibers	228.33	386.67	570	625	808.33

From the table it is obvious that the Dramix type fibers exhibit principally higher bearing capacity than that created from the fibers with rectangular shape. This is in full compliance with the numerical results.

5. CONCLUSIONS

Shape optimization of fibers in a composite structure presented in this paper is based on an original formulation of optimal shape problems leading to Euler's equations belonging to the optimization. The problems are concentrated on fiber reinforced concrete, namely to such cases where higher fiber volume ratio is required. An optimal shape design of fibers is formulated with the goal obtaining the highest bearing capacity and the minimum displacements in a unit cell. Finite element method is the numerical tool; its mesh is adapted to the current iteration step as a spring web. The examples are selected in such a way that the restriction on the possible optimum of the fiber shape is applied and one of the phases is much stiffer than the other. It appears that the assumption of stiffer fiber leads to the convex relation r and φ while if the stiffness is interchanged this relation changes to concave. These relations are very important for selecting the appropriate shapes of the phases and should be respected in the design of the composite elements. The optimization shows very important results: in details it depends on the volume ratios of both phases, but the nature of the optimal shape does not change. The optimal shapes are completely different if the fiber is much stiffer then the matrix and vice versa if the matrix is stiffer.

The results from the numerical studies of FRSC (fiber reinforced steel composites) have also partly been studied experimentally and the comparison of the results from tests and from numerical approach is reasonable.

It is necessary to note that the choice of the cost functional principally influences the optimization target. In one previous paper by the first author of this work it was shown that maximum bearing capacity is attained together with the minimum displacement field. On the other hand this approach, based on the constraint created by Lagrangian multipliers, is usable in wide range of other shape optimization procedures. One is found in Prochazka et al. (2009), other can be formulated for biomechanics, where from given material properties of all phases on micro-level and overall properties on macro-level the optimal shape can be found (keeping the effective properties in reasonable bounds, given by Hashin and Shtrikman bound estimates, for example). Next the optimal effective properties in a heat transfer problem can be solved in a similar way as in this work. The latter is a content of the paper by the authors submitted to CMES, where the boundary element method is suitable, Prochazka et al. (2012).

ACKNOWLEDGMENT

This paper was prepared under financial support of GAČR, project No. P105/10/0266.

REFERENCES

Cangiano, S., Cucitore, R. and Plizzari, G.A.: 2003, Effect of interface microstructure on the pull out behavior of steel fibres in concrete, International Conference on Advances in Concrete and Structures (ICACS 2003), Xuzhou, PR China, RILEM Proceedings 32, 1015–1022.

Kato, J. and Ramm, E.: 2010, Optimization of fiber geometry for fiber reinforced composites considering damage, Finite Elements in Analysis and Design, 46 (2010), 401–415. DOI: 10.1016/j.finel.2010.01.001

Kato, J., Lipka, A., Ramm, E.: 2009, Multiphase material optimization for fiber reinforced composites with strain softening, Structural and multidisciplinary optimization, 39(1), 63–81. DOI: 10.1007/s00158-008-0315-7

Oliver, J., Mora, D.F., Huespe, A.E. and Weber, R.: 2012, A micromorphic model for steel fiber reinforced concrete, International Journal of Solids and Structures, 49, 2990–3007. DOI: 10.1016/j.ijsolstr.2012.05.032

Prochazka, P.P., Dolezel, V. and Lok, T-S.: 2009, Optimal shape design for minimum Lagrangian, Engineering Analysis with Boundary Elements, 33, 447–455. DOI: 10.1016/j.enganabound.2008.09.003

Prochazka, P.P., Kravtsov, A.N. and Lok T-S.: 2011, Assessment of laminated cylindrical arch loaded by a shock wave, Int J. Protective Structures, 2(2), 267–282.

Prochazka, P.P. and Sejnoha, J.: 1996, Behavior of composites on bounded domain, BE Communications, 7, 6–8.

Procházka, P. and Trckova, J.: 2011, Material properties of FRC with recycled aggregate, Acta Geodyn. Geomater., 8, No. 2, 105–113.

Prochazka, P.P. and Valek, M.: 2012, Optimal shape of fibers in transmission problem, Comp. Model. Engng. and Sci. 87(3), 207–224

Valek, M.J. and Prochazka, P.P.: 2009, Overall material properties of debonding composites, CTU Prague, Czech Republic.

Suquet, P.M.: 1987, Elements of homogenization for inelastic solid mechanics. Lecture Notes in Physics 272: Homogenization Techniques for Composite Media, Eds. E. Sanches Palencia and A. Zaoui, Springer-Verlag.

Szuladzinski, G.: 2012, Does stronger concrete make stronger and more resilient elements?, Int. J. Protective Structures, 3(3), 293–310.